Transparent soil model tests on piled ground responses due to adjacent tunnelling

Xiaowan Zhou[1], W. Zhang[1,2]

[1] School of Civil Engineering, Chongqing University, Chongqing 400045, China.
[2]Key Laboratory of New Technology for Construction of Cities in Mountain Area, Chongqing University, Chongqing 400045, China

ABSTRACT

Tunnel deformation and failure mechanism are studied under the condition of different piles stiffness, which are based on the transparent soil test technology. It is concluded that the failure modes of condition one, condition two and condition three are similar with each other, which are all in the form of “funnel shape”. With the increase of drainage volume, the displacement of soil increases and the deformation range becomes wider and wider. With the decrease of pile stiffness, the anti-disturbance ability of tunnel surrounding rock decreases successively.
Keywords: transparent soil; tunnel ; pile; model test

1 INTRODUCTION

Deformation and failure evolution rules of surrounding rock have always been one of the important problems of tunnel engineering (Bromset et al. 1967; Peck 1969), and many scholars have done fruitful work (Davis et al. 1980; Clough 1983; Lee 2006; Adachi 2003; Hamid et al. 2013, 2014; Wan et al. 2016, Goh et al. 2017). Due to the restrictions of traffic routes and underground space construction and other factors, subway tunnels sometimes inevitably pass under the existing pile foundation in subway design and construction. Therefore, it has become an urgent problem to ensure the safety and stability of piled ground by tunnelling under existing pile foundation.

Traditional model test requires embedding many sensors in the soil to measure deformation, but the sensors will affect the properties of the soil, thus affecting the experimental results. In order to visualize the interior of soil mass, transparent soil test technology was proposed by Allersma (1982). Later, this technology was developed by Iskander (2002), Sade (2002), Ni (2010), Toiya (2007), Liu (2009, 2010), Siemens,G.A. (2014), Ahmed, M (2011, 2015) and other scholars.

According to model test carried out by transparent soil technology, Cao et al., (2014, 2015), Zhou et al. (2017, 2018), Kong et al. (2015) realized the visualization of soil displacement around piles under the action of pulling. Qi et al. (2015) studied the buckling of slender piles.

Sun et al. (2011) studied the internal deformation characteristics of soil mass during shield tunneling based on transparent soil model test. And they analyzed the mesoscopic mechanism of soil deformation.

Few scholars have analyzed piled ground responses due to adjacent tunnelling based on transparent soil and PIV technology. Therefore, this paper use transparent soil and PIV technology to study the deformation and failure evolution rules of soil in the condition of tunnelling under existing pile foundation.

2 INTRODUCTION OF TRANSPARENT SOIL MODEL TEST

Detailed equipment is described in the following subsections.

2.1 Model test system

The model test system consists of the optical platform, a computer, CCD high speed industrial cameras, an optical laser, the plexiglass model tanks, and PIV digital image processing software. The experimental system can simulate the deformation and failure of piled ground responses.

The optical platform is made of ferromagnetic stainless steel, with honeycomb structure on the surface of the platform. CCD high speed industrial camera has a resolution of 1280 x 960, and the computer operated camera control program can continuously capture the deformation process of surrounding rock during tunnelling. The plate optical laser model is EP532-3W, its output power is 3W, the wavelength is 532nm, the thickness of the plate light is less than 1mm, and the output Angle is 10-25 degrees. The model groove is made of acrylic plexiglass, each surface is bonded with strong adhesive, and the bottom of each surface is ribbed to restrict the deformation of the model groove. The model slot size is 320mm * 200mm * 300mm, the wall thickness is 5mm, there are 50mm model holes in front of the model slot, the hole center is 75mm from the bottom surface, and 160mm from both sides. The outside of the model hole is bonded with a 40mm long circular pipe to fix the rubber film. The size of the plate is 300mm * 160mm, and there are 5 acrylic rods in each vertical row, with the spacing of 50mm, and 2 acrylic rods in each horizontal row, with the spacing of 80mm, with a total of 10 acrylic rods. There are 65mm long acrylic rods with diameters of 6mm, 4mm and

2mm.10 acrylic rods of the same diameter are cantilevered on one plate. Three acrylic rods of different diameters are placed on three plates as shown in Fig.1. Calibration was marked on the edge of the model tank, and the position of the laser was moved to select the section for shooting. Finally, PIVview2 software is used for image processing. The test system is shown in Fig.2.

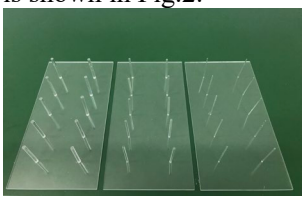

Fig. 1. Three diameters of piles

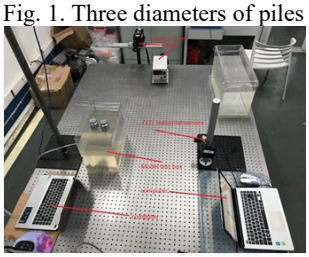

Fig. 2. Model test system

2.2 Selection and preparation of model test materials

The solid material of transparent soil adopts glass sand with particle size of 0.5-1mm. Its maximum dry density is 1.274 g/cm^3, and its minimum dry density is 0.907 g/cm^3. The pore liquid is made up of No.15 mineral white oil and n-dodecane according to the mass ratio of 4:1. The refractive index of the pore liquid is 1.4585. Transparent configuration by the method of soil and the corresponding natural sand has the similar physical and mechanical properties of graded (Kong et al. 2013) internal friction Angle range between 36 ° - 39 °. The drainage method adopted is to simulate the formation loss caused by tunnelling. The tunnel model adopts a rubber film with a diameter of 50mm, one end is tied tightly and the other end is filled with rubber plugs. The hose through the rubber plug is connected to the tap. The tunnel model is shown in Fig. 3. Before the test, the model tank should be cleaned, the tunnel model should be preset, and materials for transparent soil should be prepared.

Fig. 3. Tunnel model

Firstly, the quality of required glass sand should be weighed, the volume of glass sand in the model box should be calculated according to density. Secondly, the refraction index of No.15 mineral white oil and n-dodecane was proportionally configured to match glass sand. Finally, the weighed glass sand is slowly and evenly poured into the model tank to mix with white oil. In the configuration process, glass rods are required to slowly stir transparent soil to remove bubbles. The transparent soil is compacted to a constant compactness by means of layered compaction. The thickness of each layer is 10mm.

3 INTRODUCTION TO THE TEST PROCESS AND CONDITIONS

3.1 Test process

The deformation process of shallow buried circular tunnel without lining under the action of gravity stress field was studied experimentally. Before the experiment, the model slot was placed in an appropriate position, the camera was pointed at the cross-section of the tunnel. Relative position of the camera and model slot was adjusted to make the image clear. The intensity of laser is adjusted to form stable and clear bright spots in the transparent soil. Water in the tunnel is discharged from the tap at a constant speed to reduce the volume to simulate tunnelling, and the drainage volume is 50mL each time, as shown in Fig.4.

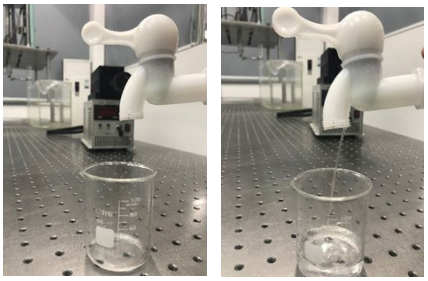

Fig. 4. Drain device

A group of photos shall be taken for each position of the laser, and the laser position shall be recycled once for each excavation, as shown in Fig.5. The photos are processed by post-processing software PIV.

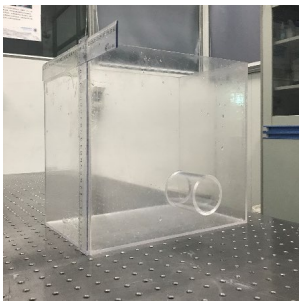

Fig. 5. Model test box

3.2 Test conditions

The shear strength of glass sand increases with the increase of relative density, and the density of the prepared transparent soil remains unchanged at 1.161 g/cm^3. According to the different diameter of pile model, it can be divided into three working conditions.

Details are shown in Table 1.

Table 1. Parameters of the transparent soil in three tests

Test No.	Relative Density (%)	pile diameter (mm)	Friction angle (°)	Minimum density ρ_{min} (g/cm^3)	Maximum density ρ_{max} (g/cm^3)	Dry density ρ (g/cm^3)
1	70	6	34	0.970	1.274	1.161
2	70	4	34	0.970	1.274	1.161
3	70	2	34	0.970	1.274	1.161

4 PIV ANALYSIS

4.1 Deformation law of soil during drainage

Analysis of soil displacement at each stage of drainage process in condition 3 are as Fig.6.

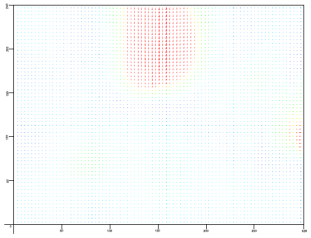

a) Displacement vector diagram of 50mL drainage

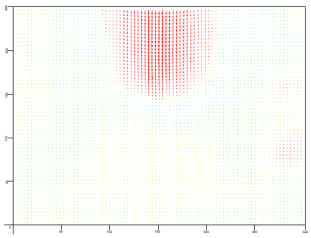

b) Displacement vector diagram of 100mL drainage

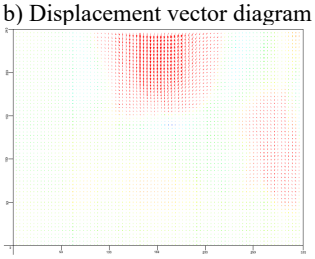

c) Displacement vector diagram of 150mL drainage

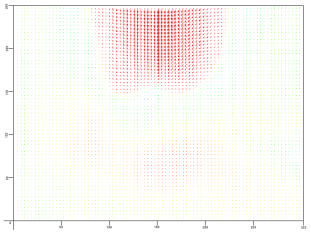

d) Displacement vector diagram of 200mL drainage

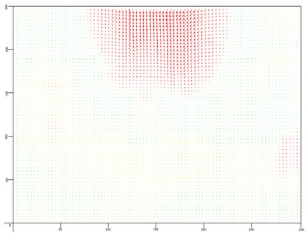

e) Displacement vector diagram of 250mL drainage

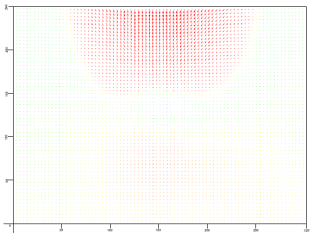

f) Displacement vector diagram of 300mL drainage

Fig.6. Displacement vector diagram of each stage in Condition 3

Fig. 5 shows the displacement vector diagram of the drainage process in condition 3, which represents the ground responds caused by volume loss. When the drainage volume is 50mL, the soil generates a small displacement. With the increase of drainage volume, the displacement of soil increases and the deformation range becomes wider and wider. When the drainage volume is 150mL, the deformation range of soil tends to be stable, forming a "funnel-shaped" failure form.

4.2 Law of soil deformation under different pile diameters

Displacement vector diagram of 150mL drainage under three conditions are as follows.

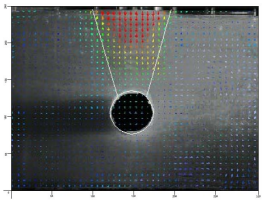

a） Condition 1

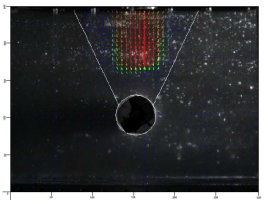

b） Condition 2

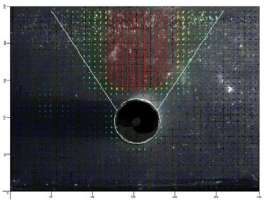

c） Condition 3

Fig. 7. Displacement vector diagram of 150mL drainage in condition 1, condition 2 and condition 3

Fig. 7 shows the displacement vector diagram under three conditions, which represents piled ground responses caused by adjacent tunnelling. In the three conditions, the deformation range tends to be stable at 150mL drainage, forming a "funnel-shaped" failure pattern. The upper surface opening in condition 1 is less than that in condition 2. The upper surface opening in condition 2 is less than that in condition 3. The above deformation process shows that when three conditions have the same drainage volume, the anti-disturbance ability of soil in condition 1, condition 2 and condition 3 becomes weaker, and the deformation range of soil in turn becomes wider. Therefore, the diameter of pile significantly influent on piled ground deformation because of tunneling under the existing pile foundation.

5 CONCLUSION

In this paper, transparent soil and PIV technology are used to simulate piled ground responses because of tunnelling under the condition of pile foundation with different diameters. The following conclusions are drawn.

1. With the increase of drainage volume, the displacement of soil increases and the deformation range becomes wider and wider. When the drainage volume is 150mL, the deformation range of soil tends to be stable, forming a "funnel-shaped" failure form.

2. The diameter of pile has a significant influence on piled ground responses due to adjacent tunnelling.

ACKNOWLEDGEMENTS

The authors are grateful to the financial support from Natural Science Foundation of Chongqing, China (cstc2018jcyjAX0632), project supported by graduate research and innovation foundation of Chongqing, China (Grant No. CYS18024) and support from the National Natural Science Foundation of China (51608071).

REFERENCES

Ahmed, M. , & Iskander, M. . (2015). Evaluation of tunnel face stability by transparent soil models. Tunnelling & Underground Space Technology Incorporating Trenchless Technology Research, 27(1), 101-110.

Adachi, T. , Kimura, M. , & Kishida, K. . (2003). Experimental study on the distribution of earth pressure and surface settlement through three-dimensional trapdoor tests. Tunnelling and Underground Space Technology incorporating Trenchless Technology Research, 18(2), 171-183.

Ahmed, M., & Iskander, M. (2011). Transparent soil model tests and fe analyses on tunnelling induced ground settlement. Geotechnical Special Publication(211), 3381-3390.

Broms, B. B. & Bennermark, H. (1967). Stability of clay at vertical openings. J. Soi/ Me& Fndn Div. Am.Sot. Civ. Engrs 93, No. SMl, 71-94 .

Changguang, Q. I. , Yonghui, C. , Xinquan, W. , Dianjun, Z. , & Architectural, F. O. . (2015). Physical modeling experiment on buckling of slender piles in transparent soil. Chinese Journal of Rock Mechanics & Engineering.

Clough,G.W.,Sweeney,S.P.&Finno,R.J.(1983).Measured soil response to EPB shield tunnelling.J.Geotech.Engng Div.,Am.Soc.Civ.Engrs 109,No.2,131-149.

Cundall, P. A., Drescher, A., & Strack, O. D. (1982). Deformation and failure of granular materials. IUTAM symposium, Delft, 1982. A.A. Balkema.

Davis,E.H.,Gunn,M.J.,Mair,R.J.&Seneviratne,H.N(1980).The stability of shallow tunnels and underground openings in cohesive material.Geotechnique 30,No.4,397-416.

Hu, C. Z., Qiang, K. G., Long, L. H., Hang, Z., & University, H. (2014). Model tests on pipe pile penetration by using transparent soils. Chinese Journal of Geotechnical Engineering, 36(8), 1564-1568.

Iskander, M. G., Liu, J., & Sadek, S. (2002). Transparent amorphous silica to model clay. Journal of Geotechnical & Geoenvironmental Engineering, 128(3), 262-273.

Ji-Zhu, S. , & Wen-Hui, X. . (2011). Design on model test of shield tunnelling in transparent soil. Journal of Wuhan University of Technology, 33(5), 108-112.

Jinyuan, L. , Zhang, C. , Yu, X. , Fu, H. , & Zhang, J. . (2009). Visualizing 3-D internal soil deformation using laser speckle and transparent soil techniques. GeoHunan International Conference, Challenges and Recent Advances in Pavement Technologies and Transportation Geotechnics, Changsha, Hunan, China, 3-6 August 2009..

Kong, G. , Cao, Z. , Zhou, H. , & Ding, X. . (2015). Experimental study on lateral bearing capacity of enlarged wedge-shaped pile using transparent soil. China Civil Engineering Journal..

KONG G Q, CAO Z H, ZHOU HANG, SUN X J. (2015).Analysis of Piles Under Oblique Pullout Load Using Transparent-Soil Models[J]. Geotechnical Testing Journal, 38(5): 728-736.

Lee, C. J. , Wu, B. R. , Chiang, K. H. , & Chen, H. T. . (2006). Tunnel stability and arching effects during tunnelling in soft clayey soil. Tunnelling & Underground Space Technology Incorporating Trenchless Technology Research, 21(2), 119-132.

Liu, J. , & Iskander, M. G. . (2010). Modelling capacity of transparent soil.(report). Revue Canadienne De Géotechnique, 47(4), 451-460.

Ni, Q. , Hird, C. C. , & Guymer, I. . (2010). Physical modelling of pile penetration in clay using transparent soil and particle image velocimetry. Géotechnique, 60(2), 121-132.

Peck, R. B. (1969). Deep excavations and tunnelling in soft ground. Proc. 7th Int. Con& Soil Mech. And Fndn Engng, Mexico, Balkema 3,225 -290.

Sadek, S. , Iskander, M. G. , & Liu, J. . (2002). Geotechnical properties of transparent silica. Canadian Geotechnical Journal, 39(1), 111-124.

Siemens, G. A., Take, W. A., & Peters, S. B. (2014). Physical and numerical modeling of infiltration including consideration of the pore-air phase 1. Canadian Geotechnical Journal, 51(12), 1475-1487.

Toiya, M. , Hettinga, J. , & Losert, W. . (2007). 3d imaging of particle motion during penetrometer testing: from microscopic to macroscopic soil mechanics. Granular Matter, 9(5), 323-329.

Zhou, H., Kong, G., CUI, Y.(2017). Model test and theoretical study on XCC pile penetration effect based on transparent soil[J]. China Civil Engineering Journal, 2017, 50(7): 100-109.

Zhou, H. , Yuan, J. , Liu, H. , & Kong, G. . (2018). Analytical model for evaluating xcc pile shaft capacity in soft soil by incorporating penetration effects. Soils & Foundations.